Resonant and Radiation Characteristics of Rectangular Microstrip Patch Antenna on Suspended-Composite Substrates

S. Bedra [1] and T. Fortaki [2]

[1] Department of Industrial Engineering
University of Khenchela, Khenchela, 40004, Algeria
bedra_sami@yahoo.fr

[2] Department of Electronics
Batna 2 University, Batna, 05000, Algeria

Abstract ─ In this paper, the resonance and radiation characteristics of rectangular microstrip patch printed on suspended and composite substrates are investigated theoretically. The analysis approach is based on the spectral-domain method of moments in conjunction with the stationary phase method. The complex resonant frequency of the microstrip antenna on suspended and composite substrates is studied with sinusoidal functions as basis functions, which show fast numerical convergence. Using a matrix representation of each layer, the far-field pattern of the suspended-composite configuration is efficiently determined by the (TM, TE) representation. The validity of the solution is tested by comparison of the computed results with experimental data. Finally, numerical results for the effects of suspended and composite substrates on the resonant frequency and half-power bandwidth are also presented.

Index Terms ─ Full-wave analysis, Galerkin method, microstrip patch, radiation pattern, suspended and composite layers.

I. INTRODUCTION

Due to their low profile, low weight, low cost and its ability of conforming to curve surfaces, conformal microstrip structures have witnessed enormous growth in the past few years [1-3]. Presently, there are many other government and commercial applications, such as mobile radio and wireless communications that have similar specifications. To meet these requirements, microstrip antennas can be used [4-5]. Since the bandwidth of microstrip antenna frequencies is very narrow [6], it is important to develop accurate algorithms for computation of those resonant frequencies [7].

The resonant frequency value of a microstrip patch antenna depends on the structural parameters and it is evident that if the resonant frequency is to be changed, a new antenna is needed. In order to achieve tunable resonant frequency characteristic, an adjustable air gap layer can be inserted between the ground plane and substrate, resulting in a two-layer structure. Using the magnetic wall cavity model, some efforts have been made to analyze microstrip antennas on suspended substrates [3, 8-10]. By means of an adjustable air gap, bandwidth enhancement is possible as a result of the lowered equivalent permittivity and the increased thickness of the structure. Therefore, a new structure having tunable properties is obtained for which a new resonant frequency formulation is required. The suspended substrate patch antenna is a special type of a patch antenna on the composite substrate [5]. In the previous literature, several researches have studied the characteristics of rectangular microstrip patch antenna with and without air gap [8-13]. Among them [9] theoretically and experimentally studied the effect of suspended substrate of the resonant frequency, but the effect of suspended substrate on the bandwidth of rectangular microstrip patch antenna was not investigated, also no results for the effects of the air gap on the radiation pattern were reported.

This paper, presents the extended spectral domain approach to study the effects of composite and suspended substrates on the resonant characteristics and radiation patterns of rectangular microstrip patch antenna.

II. PROBLEM FORMULATION

The rectangular microstrip patch antenna considered in this work is shown in Fig. 1. The antenna substrate consist of two dielectric layers (region I and II), having dielectric constant ε_{r1} and thickness d_1, and ε_{r2} and thickness d_2 respectively, and permeability μ_0 with optical axis normal to the patch. The region III is characterized by free space permeability μ_0 and permittivity ε_0. All fields and currents are time harmonic with $e^{j\omega t}$ time dependence suppressed. To simplify the analysis, the antenna feed will not be considered. The

Submitted On: October 28, 2013
Accepted On: February 24, 2016

rectangular patch is embedded in the stratification at the interface plane $z = z_p$. The transverse fields inside the composite substrate, can be obtained via the inverse vector Fourier transform as [7]:

$$\tilde{\mathbf{E}}(\mathbf{k}_s,z)=\begin{bmatrix}E_x(\mathbf{k}_s,z)\\E_y(\mathbf{k}_s,z)\end{bmatrix} = \frac{1}{4\pi^2}\int_{-\infty}^{+\infty}\int_{-\infty}^{+\infty}\bar{\mathbf{F}}(\mathbf{k}_s).\mathbf{e}(\mathbf{k}_s,z)\,dk_x\,dk_y \quad , \quad (1)$$

$$\tilde{\mathbf{H}}(\mathbf{k}_s,z)=\begin{bmatrix}H_y(\mathbf{k}_s,z)\\-H_x(\mathbf{k}_s,z)\end{bmatrix} = \frac{1}{4\pi^2}\int_{-\infty}^{+\infty}\int_{-\infty}^{+\infty}\bar{\mathbf{F}}(\mathbf{k}_s).\mathbf{h}(\mathbf{k}_s,z)\,dk_x\,dk_y \quad , \quad (2)$$

where $\bar{\mathbf{F}}(\mathbf{k}_s)$ is the kernel of the vector Fourier transform [7], and the superscripts *e* and *h* denote the *TM* and *TE* waves, respectively, and $\mathbf{k}_s = \hat{x}k_x + \hat{y}ky$ is the transverse vector wavenumber and $k_s = |\mathbf{k}_s|$:

$$\bar{\mathbf{F}}(\mathbf{k}_s)=\frac{1}{k_s}\begin{bmatrix}k_x & k_y\\k_y & -k_x\end{bmatrix}=\bar{\mathbf{F}}^{-1}(k_s), \quad (3)$$

$$\mathbf{e}(\mathbf{k}_s,z)=\begin{bmatrix}e^e(\mathbf{k}_s,z)\\e^h(\mathbf{k}_s,z)\end{bmatrix}=\bar{\mathbf{F}}(\mathbf{k}_s).\tilde{\mathbf{E}}(\mathbf{k}_s,z), \quad (4)$$

$$\mathbf{h}(\mathbf{k}_s,z)=\begin{bmatrix}h^e(\mathbf{k}_s,z)\\h^h(\mathbf{k}_s,z)\end{bmatrix}=\bar{\mathbf{F}}(\mathbf{k}_s)\cdot\tilde{\mathbf{H}}(\mathbf{k}_s,z). \quad (5)$$

The relation which related the currents $\bar{\mathbf{j}}(\mathbf{k}_s)$ on the conducting patch to the electric field in the corresponding interface ($z = z_p$) is given by:

$$\mathbf{e}(\mathbf{k}_s,z_p)=\bar{\mathbf{G}}(\mathbf{k}_s).\bar{\mathbf{j}}(\mathbf{k}_s), \quad (6)$$

where $\bar{\mathbf{G}}(\mathbf{k}_s)$ is the spectral dyadic Green's function in (TM, TE) representation, it is given by [7]:

$$\bar{\mathbf{G}}(\mathbf{k}_s)=diag\left[G^e,G^h\right]. \quad (7)$$

In the coordinate system (*x*, *y*) the dyadic Green's function $\bar{\mathbf{Q}}(\mathbf{k}_s)$ is defined by [7]:

$$\tilde{\mathbf{E}}=(\mathbf{k}_s,z_P)=\bar{\mathbf{Q}}(\mathbf{k}_s).\tilde{\mathbf{J}}(\mathbf{k}_s) = \begin{bmatrix}Q_{xx} & Q_{xy}\\Q_{yx} & Q_{yy}\end{bmatrix}.\tilde{\mathbf{J}}(\mathbf{k}_s) \quad . \quad (8)$$

Next, the Equation (8) is multiplied by $\tilde{\mathbf{F}}(\mathbf{k}_s)$. Thus, Equation (6) becomes:

$$\tilde{\mathbf{E}}(\mathbf{k}_s,z_P)=\bar{\mathbf{F}}(\mathbf{k}_s).\bar{\mathbf{G}}(\mathbf{k}_s).\bar{\mathbf{F}}(\mathbf{k}_s).\tilde{\mathbf{J}}(\mathbf{k}_s). \quad (9)$$

Comparing (8) with (9), we obtain the following relation between $\bar{\mathbf{Q}}(\mathbf{k}_s)$ and $\bar{\mathbf{G}}(\mathbf{k}_s)$:

$$\bar{\mathbf{Q}}(\mathbf{k}_s)=\bar{\mathbf{F}}(\mathbf{k}_s).\bar{\mathbf{G}}(\mathbf{k}_s).\bar{\mathbf{F}}(\mathbf{k}_s). \quad (10)$$

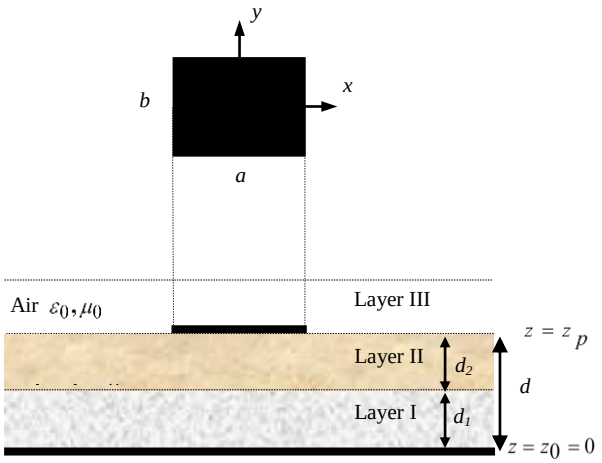

Fig. 1. Geometry of rectangular microstrip patch on suspended-composite substrates.

Now that we have the necessary Green's function, it is relatively straightforward to formulate the moment method solution for the antenna characteristics. The transverse electric field can be obtained from (8) via the inverse Fourier transform:

$$\mathbf{E}(x,y,z_p)=\frac{1}{4\pi^2}\int_{-\infty}^{+\infty}\int_{-\infty}^{+\infty}\bar{\mathbf{Q}}(\mathbf{k}_s)\cdot\tilde{\mathbf{J}}(\mathbf{k}_s)e^{(ik_xx+ik_yy)}dk_xdk_y \quad . \quad (11)$$

Enforcement of the boundary condition requiring the transverse electric field of (11) to vanish on the perfectly conducting patch yields the sought integral equation:

$$\int_{-\infty}^{+\infty}\int_{-\infty}^{+\infty}\bar{\mathbf{Q}}(\mathbf{k}_s).\tilde{\mathbf{J}}(\mathbf{k}_s)e^{(ik_xx+ik_yy)}dk_xdk_y=\mathbf{0}. \quad (12)$$

The Galerkin moment method is implemented in the Fourier transform domain to reduce the integral Equation (12) to a matrix equation. The surface current *J* on the patch is expanded into a finite series of known basis function J_{xk} and J_{ym}:

$$\mathbf{J}(x,y)=\sum_{k=1}^{K}a_k\begin{bmatrix}J_{xk}(x,y)\\0\end{bmatrix}+\sum_{m=1}^{M}b_m\begin{bmatrix}0\\J_{ym}(x,y)\end{bmatrix} \quad , \quad (13)$$

where a_k and b_m are the mode expansion coefficients to be sought. Substituting the Fourier transform of (13) into (12). Next, the resulting equation is tested by the same set of basis functions that was used in the expansion of the patch current. Thus, the integral Equation (12) is discretized into the matrix equation:

$$\begin{bmatrix} \left(\overline{\mathbf{Z}}^{11}\right)_{K\times K} & \left(\overline{\mathbf{Z}}^{12}\right)_{K\times M} \\ \left(\overline{\mathbf{Z}}^{21}\right)_{M\times K} & \left(\overline{\mathbf{Z}}^{22}\right)_{M\times M} \end{bmatrix} \cdot \begin{bmatrix} (\mathbf{a})_{K\times 1} \\ (\mathbf{b})_{M\times 1} \end{bmatrix} = \mathbf{0}, \quad (14)$$

where

$$\left(\overline{\mathbf{Z}}^{11}\right)_{qk} = \int_{-\infty}^{+\infty}\int_{-\infty}^{+\infty} Q_{xx}\, \tilde{J}_{x\,q}(-\mathbf{k}_s)\tilde{J}_{x\,k}(\mathbf{k}_s)\, dk_x dk_y, \quad (15)$$

$$\left(\overline{\mathbf{Z}}^{12}\right)_{qm} = \int_{-\infty}^{+\infty}\int_{-\infty}^{+\infty} Q_{xy}\, \tilde{J}_{x\,q}(-\mathbf{k}_s)\tilde{J}_{y\,m}(\mathbf{k}_s)\, dk_x dk_y, \quad (16)$$

$$\left(\overline{\mathbf{Z}}^{21}\right)_{lk} = \int_{-\infty}^{+\infty}\int_{-\infty}^{+\infty} Q_{yx}\, \tilde{J}_{y\,l}(-\mathbf{k}_s)\tilde{J}_{x\,k}(\mathbf{k}_s)\, dk_x dk_y, \quad (17)$$

$$\left(\overline{\mathbf{Z}}^{22}\right)_{lm} = \int_{-\infty}^{+\infty}\int_{-\infty}^{+\infty} Q_{yy}\, \tilde{J}_{y\,l}(-\mathbf{k}_s)\tilde{J}_{y\,m}(\mathbf{k}_s)\, dk_x dk_y. \quad (18)$$

The existence of non-trivial solution of (14) requires that:

$$\det(\overline{\mathbf{Z}}(f)) = 0, \quad (19)$$

where $\overline{\mathbf{Z}}$ is the matrix in (14). Equation (19) is the characteristic equation for the complex resonant frequency $f = f_r + \mathrm{i}f_i$ of the generalized microstrip structure illustrated in Fig. 1. f_r is the resonant frequency and $2f_i/f_r$ is the half-power bandwidth of the structure.

Once the complex resonant frequency is determined, the eigenvector corresponding to the minimal eigenvalue of the impedance matrix gives the coefficients of the current on the rectangular patch. The current density is thus obtained in numerical form. This current density can be used for computing the radiation electric field in the region $z \geq d$ of Fig. 1. Using the stationary phase method [7], we can obtain the far-field pattern function on the upper air half-space of Fig. 1 in terms of the transverse electric field at the plane $z = d$ as follows:

$$\begin{bmatrix} \mathbf{E}_{\theta'}(r',\theta',\phi') \\ \mathbf{E}_{\phi'}(r',\theta',\phi') \end{bmatrix} = \mathrm{i}k_0 \frac{e^{-\mathrm{i}k_0 r'}}{2\pi r'} \underbrace{\begin{bmatrix} -1 & 0 \\ 0 & \cos\theta' \end{bmatrix}}_{\mathbf{e}(\mathbf{k}_s, d)}, \quad (20)$$

where $\{r', \theta', \phi'\}$ is a local set of spherical coordinates defined with respect to the Cartesian system $\{x' \equiv x, y' \equiv y, z' \equiv z\}$ with an origin placed at the plane $z = d$ of Fig. 1.

III. RESULTS AND DISCUSSION

In this section, typical numerical results for the resonant frequencies, bandwidth and radiation patterns of rectangular patch on composite, suspended and single substrates. Although the full-wave analysis described in the previous section can give results for several resonant modes [7], only results for the TM01 mode are suggested in this paper. In order to determine the most appropriate suggestion given in the literature, we compared our computed values of the resonant frequencies and half power bandwidth of rectangular patch on single substrate with the theoretical and experimental results reported by another scientists, all which are given in Table 1 and 2. The convergence of the extended formulation of the spectral domain approach is checked by comparing our results with experimental and theoretical data available in open literature. These comparisons show that an extra improvement is obtained on the results of the previous works. Numerical results are presented for different configurations of rectangular microstrip patch antenna and compared to data available in the literature. The radiation pattern of rectangular microstrip patch antenna of suspended-composite substrates is also investigated.

The bandwidths of single layer of rectangular microstrip patch for the fundamental mode TM_{01}, computed by the present approach are depicted in Table 1. It is clear from Table 1 that, the calculated results bandwidths from the present approach are very close to experimental and theoretical values [13, 14].

In Table 2, we have compared our computed resonant frequencies values with theoretical and experimental values [9] available in the open literature for a rectangular patch without air gap layer having different parameters of antenna. The results of our approach show good consistency with both experimental and theoretical values.

Table 1: Comparison of measured and calculated bandwidth of rectangular microstrip patch antenna on single substrate, $\varepsilon_{r2} = 2.55$

Input Parameters (mm)			Bandwidth *BW* (%)		
			Measured	Calculated	
a	*b*	d_2	[13]	[14]	Present
7.76	10.8	3.3	17.50	18.48	13.10
9.87	14.5	4.5	17.90	19.17	13.18
9.74	26.20	9.52	20.60	27.17	25.7

Table 2: Comparison of calculation and measured resonant frequencies for rectangular microstrip antenna on single substrate

Input Parameters				Resonant Frequency f_r^{01} (GHz)		
				Measured	Calculated	
a (mm)	*b* (mm)	d_2 (mm)	ε_r	[15]	[9]	Present
30	20	1.27	10.2	2.26	2.29	2.29
29.83	19	2.54	10.2	2.18	2.32	2.33
40	25	0.79	2.22	3.92	3.93	3.91

In Table 3, effects of air gap layer on the resonant frequencies have been tabulated for various thickness of air gap layer. This can be obtained by having $d_1 = 0$, and $\varepsilon_{r1} = 1$.

Table 3: Computed values of resonant frequency of rectangular microstrip patch with different air gap heights, $\varepsilon_{r2} = 2.33$, $d_2 = 1.575$ mm, $a = b = 30$ mm

Air Gap Thickness d_1 (mm)	Resonant Frequency f_r^{01} (GHz)		
	Calculated [9]	Simulated [9]	Present
0	3.11	3.10	3.13
1	3.58	3.51	3.61
2	3.64	3.50	3.68

The results of the present approach show the closest agreement with calculated and simulated values [9]. In order to observe the effects suspended and composite substrates on the resonant frequencies, bandwidth and radiation pattern of rectangular microstrip antenna shown in Fig. 1, some results are presented and investigated in this section. The effect of the composite substrate to the resonance frequency and the bandwidth of the rectangular microstrip antenna are studied. In Fig. 2, we present results for resonant frequencies versus the variation of thickness d_2 of layer II of a rectangular microstrip patch on suspended-composite substrates. It is observed that the resonant frequency is increased for a composite substrate and deceased for a suspended substrate with the increase of d_2. The effect of the suspended-composite substrate to the half-power bandwidth is shown in Fig. 3. Note that the bandwidth of rectangular microstrip patch antenna increased for composite and suspended substrates, substrate with increase of d_2.

We show in Fig. 4 the equivalent relative permittivity of the composite two-layer structure, computed from [16], Equation (21), versus air separation for the structures considered in Fig. 4.

It is seen that when d_2 increases, the equivalent relative permittivity decreases rapidly for composite substrate, and increases for suspended substrate.

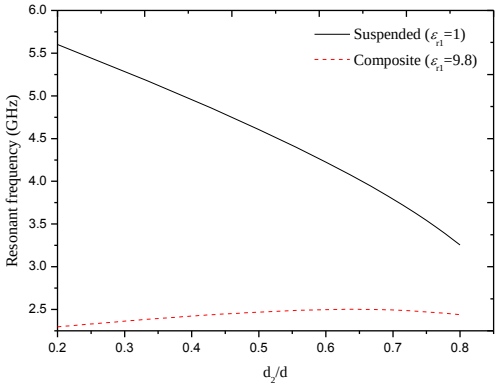

Fig. 2. Variation of the resonant frequency on suspended-composite substrates with the variation of thickness of layer II; ($d_1 = 1.27$ mm, $a = 27$ mm, $b = 22$ mm, $\varepsilon_{r2} = 5.4$).

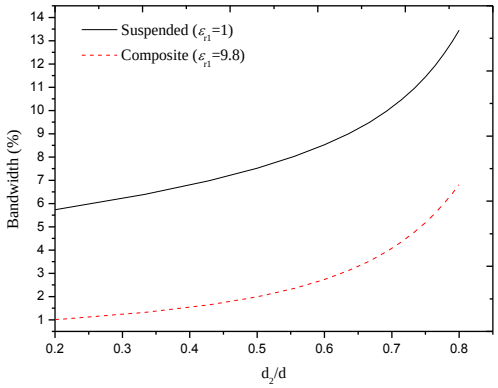

Fig. 3. Variation of the half-power bandwidth on suspended-composite substrates with different thicknesses of layer II, (parameters as in Fig. 2).

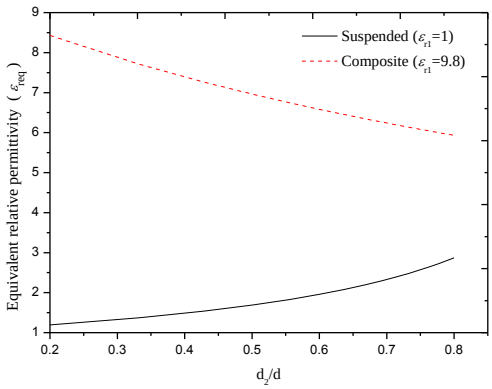

Fig. 4. Variation equivalent relative permittivity on suspended-composite substrates with different thicknesses of layer II, (parameters as in Fig. 2).

This observation can well justify the very fast decrease in the resonant frequency shown in Fig. 2. These behaviors agree with those discovered theoretically for resonant frequency and bandwidth of triangular and circular patch antenna [5, 16].

The radiation pattern of rectangular patch printed on suspended and composite substrates is investigated using the analytical technique explained in the previous section. In Figs. 5 (a) and 5 (b), we plot the variation of the normalized radiation pattern in the E-plane ($\phi = 0$) and H-plane ($\phi = \pi/2$), respectively, as function of permittivity and thickness of substrate in region II.

The three cases of single, suspended, and composite substrates are illustrated. From the results in Fig. 5 (a), it is seen that the E-plane radiation pattern is insensitive to the variation of thickness (d_2) of substrate in region II. However, the H-plane pattern show in Fig. 5 (b) exhibits important decreases (increases if $\varepsilon_{r1} = 9.8$) with increasing thickness (d_2) of substrate in region II. Thus, the directivity of the antenna increases (decreases

if $\varepsilon_{r1} = 9.8$) with the thickness (d_2) of substrate in region II.

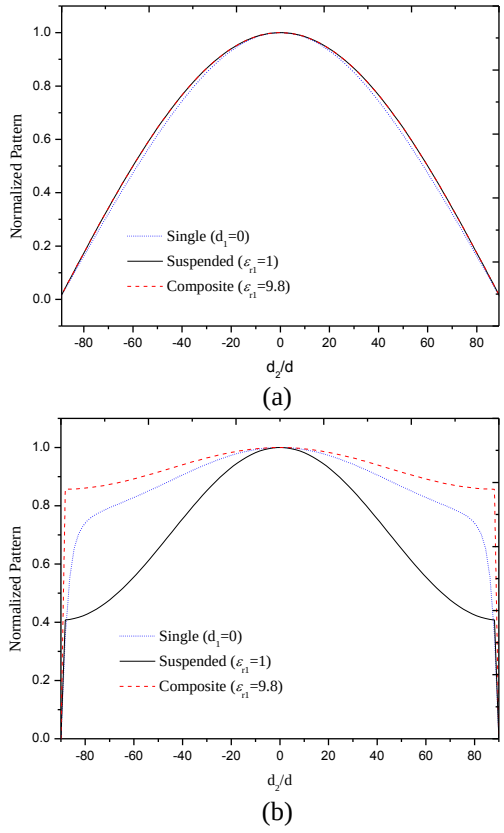

Fig. 5. Normalized radiation pattern of rectangular microstrip antennas for various configurations in the E-plane (a) and H-plane (b); a = 27 mm, b = 22 mm, d_2 = 1.27 mm, d_1 = 1.27 mm, ε_{r2} = 5.4.

To explain these results, we determine an equivalent permittivity of the composite two-layer structure by first deriving a simple approximate formula for the resonant frequency. Using (7), the spectral dyadic Green's function of the composite two-layer structure shown in Fig. 1, when d_1 and d_2 are quite thin electrically, takes the form [7]:

$$\overline{\mathbf{G}}(\mathbf{k}_s) \underset{d_1+d_2\to 0}{\to} diag\left[G^e, G^h\right]$$

$$\overline{\mathbf{G}}(\mathbf{k}_s) \underset{d_1+d_2\to 0}{\to} diag\left[k_0^2 - \frac{\varepsilon_{r1}\cdot\varepsilon_{r2}\cdot(d_1+d_2)}{\varepsilon_{r1}\cdot d_2 + \varepsilon_{r2}\cdot d_1} k_s^2, k_0^2\right] \quad (21)$$

The basis functions for the following numerical calculations are selected to be sinusoidal functions of:

$$J_{xk}(x,y) = \sin\left[\frac{k_1\pi}{a}(x+\frac{a}{2})\right] + \cos\left[\frac{k_2\pi}{b}(y+\frac{b}{2})\right], \quad (22)$$

$$J_{xk}(x,y) = \cos\left[\frac{m_1\pi}{a}(x+\frac{a}{2})\right] + \sin\left[\frac{m_2\pi}{b}(y+\frac{b}{2})\right]. \quad (23)$$

Because one sinusoidal basis function in the y direction is sufficient to give excellent convergent results, the characteristic Equation (19) reduces to:

$$\int_{-\infty}^{+\infty}\int_{-\infty}^{+\infty} \overline{\mathbf{Q}}_{yy}\tilde{\mathbf{J}}_{y1}(-\mathbf{k}_s)\,\tilde{\mathbf{J}}_{y1}(\mathbf{k}_s)\,dk_x dk_y = \mathbf{0}. \quad (24)$$

The function J_{y1} corresponds to (m_1, m_2) = (0, 1) in (23). It possesses closed-form Fourier transform, given by:

$$\tilde{J}_{y1}(\mathbf{k}_s) = \pi b \frac{\sin(k_x a/2)}{k_x} \frac{\cos(k_y b/2)}{(\pi/2)^2 - (k_y b/2)^2}. \quad (25)$$

Using the asymptotic expression of $\boldsymbol{G}$ given by Eq. (21) together with Eq. (10) and Eq. (25), and after performing some algebraic operations, Equation (24) reduces to:

$$\varepsilon_{r1}\cdot\varepsilon_{r2}\cdot(d_1+d_2)b^2k_0^2 I_1 - 4(\varepsilon_{r1}\cdot d_2 + \varepsilon_{r2}\cdot d) I_2 = 0, \quad (26)$$

where

$$I_1 = \int_0^\infty \frac{\cos^2 k_y}{\left(k_y^2 - (\pi/2)^2\right)^2 - \left(k_y b/2\right)^2} dk_y,$$

$$I_2 = \int_0^\infty \frac{k_y^2 \cos^2 k_y}{\left(k_y^2 - (\pi/2)^2\right)^2 - \left(k_y b/2\right)^2} dk_y. \quad (27)$$

Using contour integration, the integrals in Eq. (27) can be evaluated explicitly giving $I_1 = 1/\pi$ and $I_2 = \pi/4$. On using the values of I_1 and I_2 in Eq. (26), we obtain the following expression for the resonant frequency:

$$f_r = \frac{C}{\left(2b\sqrt{\varepsilon_{req}}\right)}, \quad (28)$$

where C is the velocity of light in free space, and ε_{req} is the equivalent relative permittivity of the composite two-layer structure given by:

$$\varepsilon_{req} = \frac{\varepsilon_{r1}\cdot\varepsilon_{r2}\cdot(d_1+d_2)}{\varepsilon_{r1}\cdot d_2 + \varepsilon_{r2}\cdot d_1}. \quad (29)$$

IV. CONCLUSION

In this paper, a full-wave analysis has been applied to investigate the effect of suspended and composite substrates on the radiation pattern of a rectangular microstrip antenna. The spectral-domain integral equations in conjunction with stationary phase method have been used to calculate the complex resonant frequency and radiation pattern of various antenna structures. In order to test the validity of the analysis, the numerical results obtained via Galerkin's method in the Fourier transform domain have been compared with theoretical and experimental data, and good agreement has been found. Numerical results show that the resonant frequency is increased, for suspended substrate and decreases for composite substrate, so the air separation can be adjusted to have a maximum operation frequency of the antenna.

The bandwidth, on other hand, decreases for composite, and the bandwidth is increased for suspended substrate, the E-plane radiation pattern is significantly affected, so that an enhancement in the directive gain of the antenna is achieved. The present approach is also well suited for single substrate. No experimental and theoretical values are available for a rectangular patch printed on composite substrate, only the theoretical results of suspended substrate are compared with experimental data. Note that, the theoretical results of rectangular patch microstrip antenna need to be further validated with experimental works.

REFERENCES

[1] R. Bedra, S. Bedra, S. Benkouda, and T. Fortaki, "Efficient full-wave analysis of resonant modes of circular microstrip antenna printed on isotropic or uniaxially anisotropic substrate," *Wireless Personal Communications*, vol. 81, no. 1, pp. 239-251, 2015.

[2] S. Bedra, R. Bedra, S. Benkouda, and T. Fortaki, "Efficient full-wave analysis of inverted circular microstrip antenna," *Microwave and Optical Technology Letters*, vol. 56, no. 10, pp. 2422-2425, 2014.

[3] S. Chattopadhyay, M. Biswas, J. Y. Siddiqui, and D. Guha, "Rectangular microstrips with variable air gap and varying aspect ratio: improved formulations and experiments," *Microwave and Optical Technology Letters*, vol. 51, no. 1, pp. 169-173, 2009.

[4] S. Bedra, R. Bedra, S. Benkouda, and T. Fortaki, "Full-wave analysis of anisotropic circular microstrip antenna with air gap layer," *Progress In Electromagnetics Research M*, vol. 34, pp. 143-151, 2014.

[5] M. Biswas and M. Dam, "Characteristics of equilateral triangular patch antenna on suspended and composite substrates," *Electromagnetics*, vol. 33, no. 2, pp. 99-115, 2013.

[6] V. Losada, R. R. Boix, and M. Horn, "Resonant modes of circular microstrip patches in multilayered substrate," *IEEE Trans. Antennas Propagat*., vol. 47, no. 4, pp. 488-497, 1999.

[7] T. Fortaki, D. Khedrouche, F. Bouttout, and A. Benghalia, "A numerically efficient full-wave analysis of a tunable rectangular microstrip patch," *International Journal of Electronics*, vol. 91, no. 1, pp. 57-70, 2004.

[8] F. Abboud, J. P. Damino, and A. Papiernik, "Accurate model for the input impedance of coax-fed rectangular microstrip antenna with and without air gaps," *Proc. Int. Conf. Antennas Propag*., pp. 102-106, 1989.

[9] S. Chattopadhyay, M. J. Biswas, Y. Siddiqui, and D. Guha, "Input impedance of probe-fed rectangular microstrip antennas with variable air gap and varying aspect ratio," *IET Microw. Antennas Propag*., vol. 3, no. 8, pp. 1151-1156, 2009.

[10] H. I. Kang and J. T. Song, "Electrically tunable rectangular microstrip antenna," *Electron. Lett.*, vol. 46, no. 1, pp. 18-19, 2009.

[11] I. Wolff and N. Knoppik, "Rectangular and circular microstrip disk capacitors and resonators," *IEEE Trans. Microwave Theory Tech*., vol. 22, no. 10, pp. 857-864, 1974.

[12] E. Chang, S. A. Long, and W. F. Richards, "Experimental investigation of electrically thick rectangular microstrip antennas," *IEEE Trans. Antennas Propag*., vol. 34, no. 6, pp. 767-772, 1986.

[13] M. Kara, "A novel technique to calculate the bandwidth of rectangular microstrip antenna elements with thick substrates," *Microwave and Optical Technology Letters*, vol. 12, no. 2, pp. 59-64, 1996.

[14] I. J. Bahl and P. Bhartia, *Microstrip Antennas*, Artech House, Canton, MA, 1980.

[15] D. Schaubert, D. Pozar, and A. Adrian, "Effect of microstrip antenna substrate thickness and permittivity: comparison of theories and experiment," *IEEE Trans. Antennas Propag.*, vol. 37, no. 6, pp. 677-682, 1989.

[16] N. Nasimuddin, K. Esselle, and A. K. Verma, "Fast and accurate model for circular microstrip antennas on suspended and composite substrates," *IEEE Trans. Antennas Propag*., vol. 53, no. 9, pp. 3097-3100, 2005.